# Domain textures in the fractional quantum Hall effect

**Ziyu Liu[1,*], Ursula Wurstbauer[2], Lingjie Du[3], Ken W. West[4], Loren N. Pfeiffer[4], Michael J. Manfra[5,6], Aron Pinczuk[1,7,‡]**

*[1] Department of Physics, Columbia University, New York, New York 10027, USA*

*[2] Institute of Physics, University of Münster, Wilhelm-Klemm-Str.10, 48149 Münster, Germany*

*[3] School of Physics, and National Laboratory of Solid State Microstructures, Nanjing University, Nanjing 210093, China*

*[4] Department of Electrical Engineering, Princeton University, Princeton, New Jersey 08544, USA*

*[5] Department of Physics and Astronomy, School of Materials Engineering,*

*and School of Electrical and Computer Engineering, Purdue University, Indiana 47907, USA*

*[6] Microsoft Quantum Lab Purdue, Purdue University, West Lafayette, Indiana 47907, USA*

*[7] Department of Applied Physics and Applied Mathematics, Columbia University, New York, New York 10027, USA*

**zl2577@columbia.edu, ‡ap359@columbia.edu*

**Impacts of domain textures on low-lying neutral excitations in the bulk of fractional quantum Hall effect (FQHE) systems are probed by resonant inelastic light scattering. We demonstrate that large domains of quantum fluids support long-wavelength neutral collective excitations with well-defined wave vector (momentum) dispersion that could be interpreted by theories for uniform phases. Access to dispersive low-lying neutral collective modes in large domains of FQHE fluids such as long wavelength magnetorotons at filling factor $\nu = 1/3$ offer significant experimental access to strong electron correlation physics in the FQHE.**

Current geometrical theories of strongly correlated phases in fractional quantum Hall effect (FQHE) fluids of two-dimensional electron systems (2DES) identify low-lying neutral collective excitations (known as magnetorotons [1]) as chiral gravitons [2–7]. The bulk of FQHE fluids is non-uniform and formation of domain textures [8–11] have significant impact on low-lying collective excitations [12–14]. The impact of bulk domain textures in strongly correlated phases is the subject of increasing attention, with prominent examples in FQHE fluids [15–20] and in high temperature superconductors [21–24]. To investigate the insulating bulk of quantum Hall phases, studies on thermal transport and electronic interference by edge modes are interpreted under bulk-edge correspondence [25–31]. Experimental methods that directly probe low-lying neutral collective excitations in the bulk of FQHE fluids are crucial tools in the quest to understand strong electron correlation physics.

In the second Landau level (SLL) at $\nu = 7/3$ a seemingly conventional FQHE is actually very distinct from its counterpart at $\nu = 1/3$ in the lowest Landau level (LLL) [32–38]. Even under a small in-plane magnetic field, appearance of anisotropic longitudinal resistance indicates emergence of domains of nematic phases [39,40] that coexist with domains of the bulk FQHE fluid [41]. Newly discovered collective modes under a small in-plane magnetic field are interpreted as long-wavelength plasmons of nematic domains in the filling factor range $2 < \nu < 3$ [42]. Studies of the plasmons under a small in-plane magnetic field serve as a probe of the impact of domain textures on low-lying collective excitations.

Access to magnetoroton modes of FQHE fluids and to plasmons of nematic liquids is provided by resonant inelastic light scattering (RILS) methods [13,42]. Here we report that RILS by nematic plasmons at $\nu = 7/3$ under a small in-plane magnetic field reveals a wide range of nematic domain sizes from around 1 $\mu m$ to characteristic sizes larger than several microns, and establishes FQHE-nematic fluids at $\nu = 7/3$ as an ideal platform to study impacts of domain textures on low-lying neutral excitations. The domains with dimensions much larger than the inelastic scattering wavelength (about 1 $\mu m$) support low-lying collective excitations with well-defined wave vector (momentum) dispersions. Very sharp dispersive long-wavelength magnetoroton modes have been reported in the LLL at $\nu = 1/3$ [13]. We surmise that the observed modes, with well-defined wave vectors, are excitations of the FQHE fluid in large domains. Results at $\nu = 1/3$ reported in previous works are examined to highlight possible experimental insights on long-wavelength magnetoroton excitations that are identified as chiral gravitons under strong electron correlation in recent theory for uniform FQHE phases [4–7].

Characteristic domain sizes are obtained by modelling the RILS intensity of nematic plasmons. While the matrix element depends on plasmon-electron interactions [12], we focus here on the photon frequency dependence and on breakdown of wave vector conservation due to formation of domain textures. We find that intensity is [43]:

$$I \propto \left|\frac{1}{(\omega_I-\omega_1-i\gamma_1)}\frac{1}{(\omega_o-\omega_2-i\gamma_2)}\right|^2 \frac{1}{(\omega(q)-\omega(k))^2+(\Delta\omega/2)^2} \qquad (1)$$

$\omega_1$ ($\omega_2$) and $\gamma_1$ ($\gamma_2$) are the energies and broadenings of the incoming (outgoing) resonant channels of optical excitations of the GaAs quantum well that hosts 2DES. When both incoming ($\omega_I$) and outgoing ($\omega_o$) photon energies are in the vicinity of these optical excitations, a large intensity enhancement occurs through double resonant inelastic light scattering (DRILS). $\omega(q)$ is the plasmon energy at wave vector $q$ [43]. Energy conservation in inelastic scattering requires $\omega(q) = \omega_I - \omega_o$. $\Delta\omega$ is the range of the plasmon energies due to breakdown of wave vector conservation.

The inelastic scattering wave vector $\boldsymbol{k}$ is along the in-plane magnetic field [42]. Wave vector conservation ($\boldsymbol{k} = \boldsymbol{q}$) occurs for domain sizes $D \gg \lambda = 2\pi/k$, where $\lambda$ is the inelastic scattering wavelength, $k = |\boldsymbol{k}|$ and $D$ is a characteristic length of nematic domains along the direction of $\boldsymbol{q}$. Wave vector conservation is broken under a finite domain size, so mode wave vectors have an uncertainty $\Delta q = 2\pi/D$ [49]. We have

$$\Delta q = \left(\frac{dq}{d\omega}\right)|_{q=k}\,\Delta\omega = 2k\Delta\omega/\omega(k) \qquad (2)$$

for nematic plasmons with dispersion $\omega(q)$ [43]. Estimates of values of $D$ can be obtained with Eq. (2) and determinations of $\Delta\omega$ from inelastic light scattering spectra.

At $\nu = 7/3$ there is a set of DRILS spectra for which breakdown of wave vector conservation has very minor impact. Here estimated nematic domain sizes are $D \approx 5.3\ \mu m \gg \lambda = 1.2\ \mu m$. In the same device, strong impact of breakdown of wave vector conservation in another set of spectra is

found for domains that have $D$ comparable to $\lambda$. The optical resonances in large nematic domains involve quasiparticle states close to the Fermi level. This could be evidence showing that large nematic domains are responsible for anisotropic electrical conduction in the FQHE at $\nu = 7/3$ under tilted magnetic fields [41]. Domains of FQHE fluid with $D > \lambda$ and those with $D < \lambda$ should coexist in the non-uniform bulk of FQHE states. Albeit the non-uniformity, low-lying neutral collective excitations in large domains with $D \gg \lambda$ accessed by RILS and DRILS would manifest the fundamental correlation physics in the uniform bulk of FQHE phases in the LLL and the SLL.

The ultraclean 2DES is confined in a 30-nm-wide, symmetric, modulation-doped single GaAs/AlGaAs quantum well. Carrier mobility of the wafer measured by transport is $\mu = 23.9 \times 10^6$ cm$^2$/Vs at 300 mK. The sample is mounted on the cold finger of a $^3$He/$^4$He-dilution refrigerator with windows for direct optical access and inserted in the bore of a 16T superconducting magnet. All measurements were performed at T $\leq$ 45 mK. The electron density under illumination is directly determined in each cool down by RILS measurements of spin waves at $\nu = 3$ (Fig. S2) and yields $n = 2.8 \times 10^{15}$ m$^{-2}$ [43]. The stability of electron density and sample quality against illumination are confirmed by photoluminescence (PL) and RILS measurements under zero magnetic field [43]. Figure 1(a) describes the back-scattering geometry at a small tilt angle $\theta = 20^o$. The finite wave vector transfer in back-scattering is $k = |\boldsymbol{k_I} - \boldsymbol{k_o}|sin\theta$, where $\boldsymbol{k_I}$ and $\boldsymbol{k_o}$ are wave vectors of the incoming and outgoing photons. DRILS spectra are excited with the linearly polarized tunable emission from a Ti:sapphire laser that is finely tuned to match the $\omega_1$ excitation. The incident power density was kept well below $10^{-4}$ W/cm$^2$. The outgoing photons are dispersed by a triple grating spectrometer and recorded by a CCD camera.

Optical excitons contributing to the DRILS matrix element are built from transitions between quasiparticles in conduction states and holes in valence states shown in steps 1 and 3 in Figs. 1(b) and 1(c). These resonant channels are identified from PL and resonant Rayleigh scattering spectra at $\nu = 7/3$ as shown in Fig. S1 [43]. At $\nu = 7/3$ excitons participating in DRILS are extremely sharp, indicating that Landau levels in the bulk of nematic-FQHE fluid system support well-defined states even under non-uniform conditions that must prevail due to coexistence of two distinct phases (the FQHE fluid and the nematic liquid). FQHE fluid at $\nu = 7/3$ is characterized by the determination of low energy magnetoroton excitations, which is suppressed by increasing temperatures or deviation of filling factors (Fig. S3) [43,46].

Two types of DRILS spectra of plasmons are reported. They are defined by the outgoing resonances in steps 3 shown in Figs. 1(b) and 1(c). In Low Outgoing Resonance (LOR) mode the outgoing photon resonates with $L$ transitions that involve states of correlated quantum fluids in the SLL [50]. In High Outgoing Resonance (HOR) mode the outgoing photon resonates with the excitonic $X$ transition involving empty states in the partially populated SLL [50]. Figures 2 and 3 report DRILS results by nematic plasmons at $\nu = 7/3$.

In results for DRILS-LOR shown in Fig. 2(a) there is a sharp nematic plasmon peak that slightly blueshifts with higher incoming photon energies within the small energy range $\Delta\omega_S$. The small blueshift is due to minor impact of breakdown of wave vector conservation. Figure 2(b) plots the intensities of plasmons as a function of outgoing (red dots) or incoming (blue dots) photon

energies. The blue dots indicate a clear incoming resonance with the $X$ exciton, and the red dots indicate an outgoing resonance associated with the Fermi level of correlated phases [near the high energy edge of $L$ emission in Fig. 2(b)]. We expect the DRILS matrix element to be prominent when symmetry of the final state in $L$ is connected to $X$ exciton through plasmon-electron interactions. The sharp exciton in the outgoing resonance in LOR provides critical spectroscopic insight into links of large nematic domains with the Fermi level of 2DES. The results reveal interplays of topological order in the FQHE with nematic order that could impact anisotropic transport by edge modes [41].

In LOR, an additional broad continuum with energy range $\Delta\omega_B$ shown in Fig. 2(a) is weakly excited without double resonance. We find that in HOR this continuum of modes is DRILS active and gives rise to a series of plasmon modes within $\Delta\omega_B$ shown in Fig. 3(a). Different energy ranges of double resonant plasmons in LOR and HOR spectra reveal a rich set of domain sizes. As domain sizes increase ($D \gg \lambda$), the wave vector dispersions of elementary excitations would tend to be similar to those of a uniform electron fluid.

Modeling DRILS spectra with Eqs. (1) and (2) yields nematic domain sizes $D_S \approx 5.3\ \mu m$ in LOR and $D_B < 2.2\ \mu m$ in HOR [43]. Figure 2(c) displays nematic plasmons generated by DRILS model in LOR. Figures 2(d) and 3(b) show DRILS model fits of plasmon energies and intensities as a function of incoming photon energies in LOR and HOR, which are the two factors directly capturing the resonance evolution of plasmons. The fits successfully reproduce DRILS-LOR results. It supports the interpretation that LOR spectra are from large nematic domains with small impact of breakdown of wave vector conservation and thus represent well-defined bulk-like collective modes. In contrast, the HOR incoming resonance [Fig. 3(b)] has a flatter top with a few outliers. When domain sizes are comparable to the inelastic scattering wavelength $\lambda = 1.2\ \mu m$, wave vectors are no longer good quantum numbers and modeling of DRILS spectra may have to be modified.

It is highly significant that DRILS-LOR involves larger domains where quantum fluids with a sharp optical transition at the Fermi level are better defined. In contrast, DRILS-HOR involves intermediate states of electron-hole pairs forming $X$ and $X+$ excitons which are associated with empty states in the partially populated SLL. As a result, LOR and HOR effectively probe plasmons in two different ranges of nematic domain sizes: larger domains close to the Fermi level in LOR, and smaller domains producing stronger impact of breakdown of wave vector conservation in HOR [Fig. 1(d)]. FQHE-nematic fluids at $\nu = 7/3$ with DRILS-active plasmons thus clearly reveal distinct impacts of domain textures depending on their sizes.

Domain textures at other filling factors can also be resolved by DRILS. Figure 4(a) shows strong nematic plasmons of a non-FQHE state at $\nu = 2.68$. DRILS model reproduces main resonance features, as shown in Fig. 4(b). Compared to $\nu = 7/3$ in LOR, the broader resonance reveals smaller domain sizes $D \approx 3.5\ \mu m$, which exerts a larger impact of breakdown of wave vector conservation and is consistent with higher disorder level in the upper half of the SLL.

Large domains of FQHE fluids support neutral collective excitations with well-defined wave vector dispersion that could be observed in RILS and DRILS spectra which access bulk states.

Extremely sharp long-wavelength magnetoroton excitations at $\nu = 1/3$ were observed [13,51]. Single resonance is considered here due to the lack of a pair of well-understood resonant channels with energy difference matching the magnetoroton energy. The narrow linewidth can be regarded as a consequence of very small breakdown of wave vector conservation in RILS spectra from large domains of the bulk FQHE fluid and the small curvature of the magnetoroton dispersion near zero momentum. The low-lying neutral collective excitations from bulk-like FQHE fluid in large domains could be interpreted in terms of theories for uniform FQHE phases. With increasing wave vectors, dispersive long-wavelength modes observed in RILS at $\nu = 1/3$ split in a manner consistent with a two-roton bound state [13].

Long-wavelength magnetoroton excitations play key roles in recent geometrical theories of electron correlation in bulk FQHE phases [2,3]. Magnetoroton modes occur here as spin 2 chiral gravitons, corresponding to the long-wavelength quantum fluctuations of an internal dynamic metric [4–7]. At $\nu = 1/3$ only the mode with spin S = -2 is active in RILS experiments in the $k \to 0$ limit [4–6]. The results in Ref. 13 that reveal a magnetoroton doublet offer a key experimental insight that needs to be interpreted. In the framework of geometrical theories, a doublet may occur in RILS spectra at finite $k$ because of coupling between magnetorotons with S = -2 and +2 [4,6].

In summary, RILS and DRILS methods investigate impacts of domain textures on low-lying collective excitations in the non-uniform bulk of FQHE of 2DES in GaAs quantum structures. For domains larger than the inelastic light scattering wavelength ($\lambda = 1.2\ \mu m$) there is nearly full conservation of wave vector in the light scattering events. Magnetoroton excitations have been identified in RILS spectra from $\nu = 5/2$ FQHE fluids [45]. RILS measurements with higher resolution in large domains of FQHE fluids at $\nu = 5/2$ could identify narrow long-wavelength neutral collective excitations with well-defined wave vector dispersion. Such experiments may reveal features of topological domain textures involving Pfaffian and anti-Pfaffian orders [15–20]. Suitable design of GaAs quantum structures [28], enhanced growth protocols [52] and characterization by RILS and DRILS may lead to creation and identification of large domains of quantum fluids likely to host novel electron correlation effects.

## Acknowledgment

A. P. gratefully acknowledges illuminating discussions with F. D. M. Haldane, J. K. Jain, D. X. Nguyen, E. Rezayi and K. Yang. Z. L. gratefully acknowledges valuable discussions with D. X. Nguyen and K. Yang.
The work at Columbia University was supported by the National Science Foundation, Division of Materials Research under awards DMR-1306976 and DMR-2103965. The Alexander von Humboldt Foundation partially supported the experimental work at Columbia University. U.W. acknowledges funding by the Deutsche Forschungsgemeinschaft (DFG, German Research Foundation) under projects Wu 637/4-1, 4-2, 7-1. The work at Nanjing University was supported by the Fundamental Research Funds for the Central Universities (Grant No. 14380146) and National Natural Science Foundation of China (Grant No. 12074177). The work at Purdue University is supported by the U.S. Department of Energy grant DE-SC0020138 under the QIS Next Generation Quantum Systems program. The research at Princeton University is funded in part by the Gordon

and Betty Moore Foundation's EPiQS Initiative, Grant GBMF9615 to L. N. Pfeiffer, and by the National Science Foundation MRSEC grant DMR-1420541.

## References

[1] S. M. Girvin, A. H. MacDonald, and P. M. Platzman, *Magneto-Roton Theory of Collective Excitations in the Fractional Quantum Hall Effect*, Phys. Rev. B **33**, 2481 (1986).

[2] F. D. M. Haldane, *Geometrical Description of the Fractional Quantum Hall Effect*, Phys. Rev. Lett. **107**, (2011).

[3] D. T. Son, *Newton-Cartan Geometry and the Quantum Hall Effect*, ArXiv:1306.0638 (2013).

[4] S. Golkar, D. X. Nguyen, and D. T. Son, *Spectral Sum Rules and Magneto-Roton as Emergent Graviton in Fractional Quantum Hall Effect*, J. High Energy Phys. 01 (2016).

[5] S.-F. Liou, F. D. M. Haldane, K. Yang, and E. H. Rezayi, *Chiral Gravitons in Fractional Quantum Hall Liquids*, Phys. Rev. Lett. **123**, 146801 (2019).

[6] D. X. Nguyen and D. T. Son, *Probing the Spin Structure of the Fractional Quantum Hall Magnetoroton with Polarized Raman Scattering*, Phys. Rev. Res. **3**, 023040 (2021).

[7] F. D. M. Haldane, E. H. Rezayi, and K. Yang, *Graviton Chirality and Topological Order in the Half-Filled Landau Level*, ArXiv:2103.11019 (2021).

[8] V. Venkatachalam, A. Yacoby, L. Pfeiffer, and K. West, *Local Charge of the ν = 5/2 Fractional Quantum Hall State*, Nature **469**, 185 (2011).

[9] J. Hayakawa, K. Muraki, and G. Yusa, *Real-Space Imaging of Fractional Quantum Hall Liquids*, Nat. Nanotechnol. **8**, 31 (2013).

[10] B. Friess, V. Umansky, L. Tiemann, K. von Klitzing, and J. H. Smet, *Probing the Microscopic Structure of the Stripe Phase at Filling Factor 5/2*, Phys. Rev. Lett. **113**, 076803 (2014).

[11] B. Friess, Y. Peng, B. Rosenow, F. von Oppen, V. Umansky, K. von Klitzing, and J. H. Smet, *Negative Permittivity in Bubble and Stripe Phases*, Nat. Phys. **13**, 1124 (2017).

[12] C. F. Hirjibehedin, I. Dujovne, I. Bar-Joseph, A. Pinczuk, B. S. Dennis, L. N. Pfeiffer, and K. W. West, *Resonant Enhancement of Inelastic Light Scattering in the Fractional Quantum Hall Regime at ν = 1/3*, Solid State Commun. **127**, 799 (2003).

[13] C. F. Hirjibehedin, I. Dujovne, A. Pinczuk, B. S. Dennis, L. N. Pfeiffer, and K. W. West, *Splitting of Long-Wavelength Modes of the Fractional Quantum Hall Liquid at ν = 1/3*, Phys. Rev. Lett. **95**, 066803 (2005).

[14] I. V. Kukushkin, J. H. Smet, V. W. Scarola, V. Umansky, and K. von Klitzing, *Dispersion of the Excitations of Fractional Quantum Hall States*, Science **324**, 1044 (2009).

[15] D. F. Mross, Y. Oreg, A. Stern, G. Margalit, and M. Heiblum, *Theory of Disorder-Induced Half-Integer Thermal Hall Conductance*, Phys. Rev. Lett. **121**, 026801 (2018).

[16] C. Wang, A. Vishwanath, and B. I. Halperin, *Topological Order from Disorder and the Quantized Hall Thermal Metal: Possible Applications to the ν = 5/2 State*, Phys. Rev. B **98**, 045112 (2018).

[17] S. H. Simon, M. Ippoliti, M. P. Zaletel, and E. H. Rezayi, *Energetics of Pfaffian–Anti-Pfaffian Domains*, Phys. Rev. B **101**, 041302(R) (2020).

[18] S. H. Simon and B. Rosenow, *Partial Equilibration of the Anti-Pfaffian Edge Due to Majorana Disorder*, Phys. Rev. Lett. **124**, 126801 (2020).

[19] W. Zhu, D. N. Sheng, and K. Yang, *Topological Interface between Pfaffian and Anti-Pfaffian Order in ν = 5/2 Quantum Hall Effect*, Phys. Rev. Lett. **125**, 146802 (2020).

[20] I. C. Fulga, Y. Oreg, A. D. Mirlin, A. Stern, and D. F. Mross, *Temperature Enhancement of Thermal Hall Conductance Quantization*, Phys. Rev. Lett. **125**, 236802 (2020).

[21] J. M. Tranquada, B. J. Sternllebt, J. D. Axe, Y. Nakamurat, and S. Uchldat, *Evidence for Stripe Correlations of Spins and Holes in Copper Oxide Superconductors*, Nature **375**, 561 (1995).

[22] V. Hinkov, D. Haug, B. Fauque, P. Bourges, Y. Sidis, A. Ivanov, C. Bernhard, C. T. Lin, and B. Keimer, *Electronic Liquid Crystal State in the High-Temperature Superconductor YBa2Cu3O6.45*, Science **319**, 597 (2008).

[23] E. H. da Silva Neto, P. Aynajian, A. Frano, R. Comin, E. Schierle, E. Weschke, A. Gyenis, J. Wen, J. Schneeloch, Z. Xu, S. Ono, G. Gu, M. Le Tacon, and A. Yazdani, *Ubiquitous Interplay Between Charge Ordering and High-Temperature Superconductivity in Cuprates*, Science **343**, 393 (2014).

[24] F. Boschini, M. Minola, R. Sutarto, E. Schierle, M. Bluschke, S. Das, Y. Yang, M. Michiardi, Y. C. Shao, X. Feng, S. Ono, R. D. Zhong, J. A. Schneeloch, G. D. Gu, E. Weschke, F. He, Y. D. Chuang, B. Keimer, A. Damascelli, A. Frano, and E. H. da Silva Neto, *Dynamic Electron Correlations with Charge Order Wavelength along All Directions in the Copper Oxide Plane*, Nat. Commun. **12**, 597 (2021).

[25] M. Banerjee, M. Heiblum, V. Umansky, D. E. Feldman, Y. Oreg, and A. Stern, *Observation of Half-Integer Thermal Hall Conductance*, Nature **559**, 205 (2018).

[26] R. L. Willett, K. Shtengel, C. Nayak, L. N. Pfeiffer, Y. J. Chung, M. L. Peabody, K. W. Baldwin, and K. W. West, *Interference Measurements of Non-Abelian e/4 & Abelian e/2 Quasiparticle Braiding*, ArXiv:1905.10248 (2019).

[27] M. Heiblum and D. E. Feldman, *Edge Probes of Topological Order*, Int. J. Mod. Phys. A **35**, 2030009 (2020).

[28] J. Nakamura, S. Liang, G. C. Gardner, and M. J. Manfra, *Direct Observation of Anyonic Braiding Statistics*, Nat. Phys. **16**, 931 (2020).

[29] B. Dutta, W. Yang, R. A. Melcer, H. K. Kundu, M. Heiblum, Y. Oreg, A. Stern, and D. Mross, *Novel Method Distinguishing between Competing Topological Orders*, ArXiv:2101.01419 (2021).

[30] D. E. Feldman and B. I. Halperin, *Fractional Charge and Fractional Statistics in the Quantum Hall Effects*, ArXiv:2102.08998 (2021).

[31] M. Yutushui, A. Stern, and D. F. Mross, *Identifying the ν = 5/2 Topological Order through Charge Transport Measurements*, ArXiv:2106.07667 (2021).

[32] C. R. Dean, B. A. Piot, P. Hayden, S. Das Sarma, G. Gervais, L. N. Pfeiffer, and K. W. West, *Contrasting Behavior of the 5/2 and 7/3 Fractional Quantum Hall Effect in a Tilted Field*, Phys. Rev. Lett. **101**, 186806 (2008).

[33] C. Zhang, T. Knuuttila, Y. Dai, R. R. Du, L. N. Pfeiffer, and K. W. West, *ν = 5/2 Fractional Quantum Hall Effect at 10T: Implications for the Pfaffian State*, Phys. Rev. Lett. **104**, 166801 (2010).

[34] J. Xia, V. Cvicek, J. P. Eisenstein, L. N. Pfeiffer, and K. W. West, *Tilt-Induced Anisotropic to Isotropic Phase Transition at ν = 5/2*, Phys. Rev. Lett. **105**, 176807 (2010).

[35] A. C. Balram, Y.-H. Wu, G. J. Sreejith, A. Wójs, and J. K. Jain, *Role of Exciton Screening in the 7/3 Fractional Quantum Hall Effect*, Phys. Rev. Lett. **110**, 186801 (2013).

[36] B. A. Schmidt, K. Bennaceur, S. Bilodeau, G. Gervais, L. N. Pfeiffer, and K. W. West, *Second Landau Level Fractional Quantum Hall Effects in the Corbino Geometry*, Solid State Commun. **217**, 1 (2015).

[37] T. Jolicoeur, *Shape of the Magnetoroton at ν = 1/3 and ν = 7/3 in Real Samples*, Phys. Rev. B **95**, 075201 (2017).

[38] H. M. Yoo, K. W. Baldwin, K. West, L. Pfeiffer, and R. C. Ashoori, *Spin Phase Diagram of the Interacting Quantum Hall Liquid*, Nat. Phys. **16**, 1022 (2020).

[39] W. Pan, R. R. Du, H. L. Stormer, D. C. Tsui, L. N. Pfeiffer, K. W. Baldwin, and K. W. West, *Strongly Anisotropic Electronic Transport at Landau Level Filling Factor 9/2 and 5/2 under a Tilted Magnetic Field*, Phys. Rev. Lett. **83**, 820 (1999).

[40] M. P. Lilly, K. B. Cooper, J. P. Eisenstein, L. N. Pfeiffer, and K. W. West, *Anisotropic States of Two-Dimensional Electron Systems in High Landau Levels: Effect of an In-Plane Magnetic Field*, Phys. Rev. Lett. **83**, 824 (1999).

[41] J. Xia, J. P. Eisenstein, L. N. Pfeiffer, and K. W. West, *Evidence for a Fractionally Quantized Hall State with Anisotropic Longitudinal Transport*, Nat. Phys. **7**, 845 (2011).

[42] L. Du, U. Wurstbauer, K. W. West, L. N. Pfeiffer, S. Fallahi, G. C. Gardner, M. J. Manfra, and A. Pinczuk, *Observation of New Plasmons in the Fractional Quantum Hall Effect: Interplay of Topological and Nematic Orders*, Sci. Adv. **5**, eaav3407 (2019).

[43] See Supplemental Material [url] for optical transitions in the second Landau level, experimental details on determining the filling factors, characterization of the FQHE state, the model of doubly resonant inelastic light scattering intensity and its quantitative analysis, which includes Refs. [44-48].

[44] T. D. Rhone, J. Yan, Y. Gallais, A. Pinczuk, L. Pfeiffer, and K. West, *Rapid Collapse of Spin Waves in Nonuniform Phases of the Second Landau Level*, Physical Review Letters **106**, 196805 (2011).

[45] U. Wurstbauer, K. W. West, L. N. Pfeiffer, and A. Pinczuk, *Resonant Inelastic Light Scattering Investigation of Low-Lying Gapped Excitations in the Quantum Fluid at ν = 5/2*, Physical Review Letters **110**, 026801 (2013).

[46] U. Wurstbauer, A. L. Levy, A. Pinczuk, K. W. West, L. N. Pfeiffer, M. J. Manfra, G. C. Gardner, and J. D. Watson, *Gapped Excitations of Unconventional Fractional Quantum Hall Effect States in the Second Landau Level*, Physical Review B **92**, 241407(R) (2015).

[47] Y. Gallais, J. Yan, A. Pinczuk, L. N. Pfeiffer, and K. W. West, *Soft Spin Wave near N=1: Evidence for a Magnetic Instability in Skyrmion Systems*, Physical Review Letters **100**, 086806 (2008).

[48] T. D. Rhone, D. Majumder, B. S. Dennis, C. Hirjibehedin, I. Dujovne, J. G. Groshaus, Y. Gallais, J. K. Jain, S. S. Mandal, A. Pinczuk, L. Pfeiffer, and K. West, *Higher-Energy Composite Fermion Levels in the Fractional Quantum Hall Effect*, Physical Review Letters **106**, 096803 (2011).

[49] R. Shuker and R. W. Gammon, *Raman-Scattering Selection-Rule Breaking and the Density of States in Amorphous Materials*, Phys. Rev. Lett. **25**, 222 (1970).

[50] A. L. Levy, U. Wurstbauer, Y. Y. Kuznetsova, A. Pinczuk, L. N. Pfeiffer, K. W. West, M. J. Manfra, G. C. Gardner, and J. D. Watson, *Optical Emission Spectroscopy Study of Competing Phases of Electrons in the Second Landau Level*, Phys. Rev. Lett. **116**, 016801 (2016).

[51] A. Pinczuk, B. S. Dennis, L. N. Pfeiffer, and K. West, *Observation of Collective Excitations in the Fractional Quantum Hall Effect*, Phys. Rev. Lett. **70**, 3983 (1993).

[52] Y. J. Chung, K. A. Villegas Rosales, K. W. Baldwin, P. T. Madathil, K. W. West, M. Shayegan, and L. N. Pfeiffer, *Ultra-High-Quality Two-Dimensional Electron Systems*, Nat. Mater. **20**, 632 (2021).

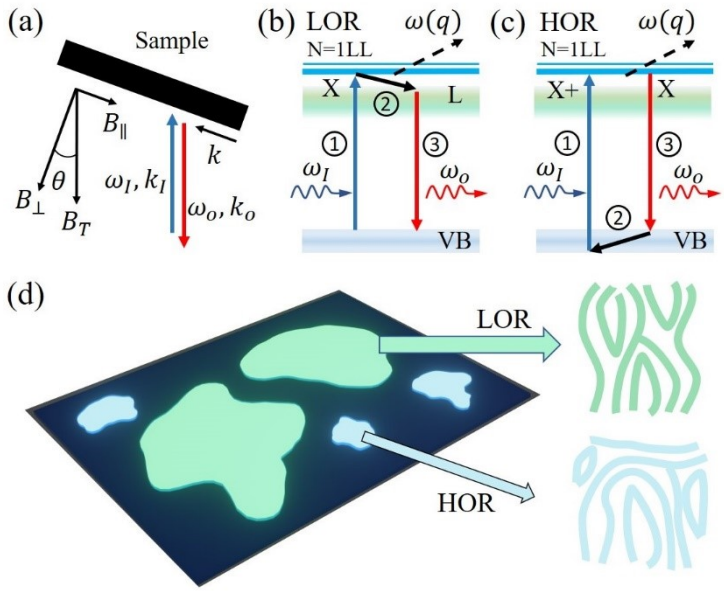


FIG. 1 (color online). (a) Schematic description of the experimental back-scattering geometry at a tilt angle $\theta = 20^o$. Incoming and outgoing photons have energies $\omega_I$, $\omega_o$ and wave vectors $k_I$, $k_o$, respectively. The total magnetic field $B_T$ produces a perpendicular component $B_\perp$ and a parallel component $B_\parallel$. The inelastic scattering wave vector is parallel to $B_\parallel$. (b)(c) Different DRILS processes between valence bands and the SLL in (b) LOR and (c) HOR. A plasmon mode $\omega(q)$ is generated in the second step. (d) Schematic plot of domain textures probed by DRILS in nematic-FQHE fluids. Large (small) nematic domains are active in LOR (HOR). Smaller domains are more disordered.

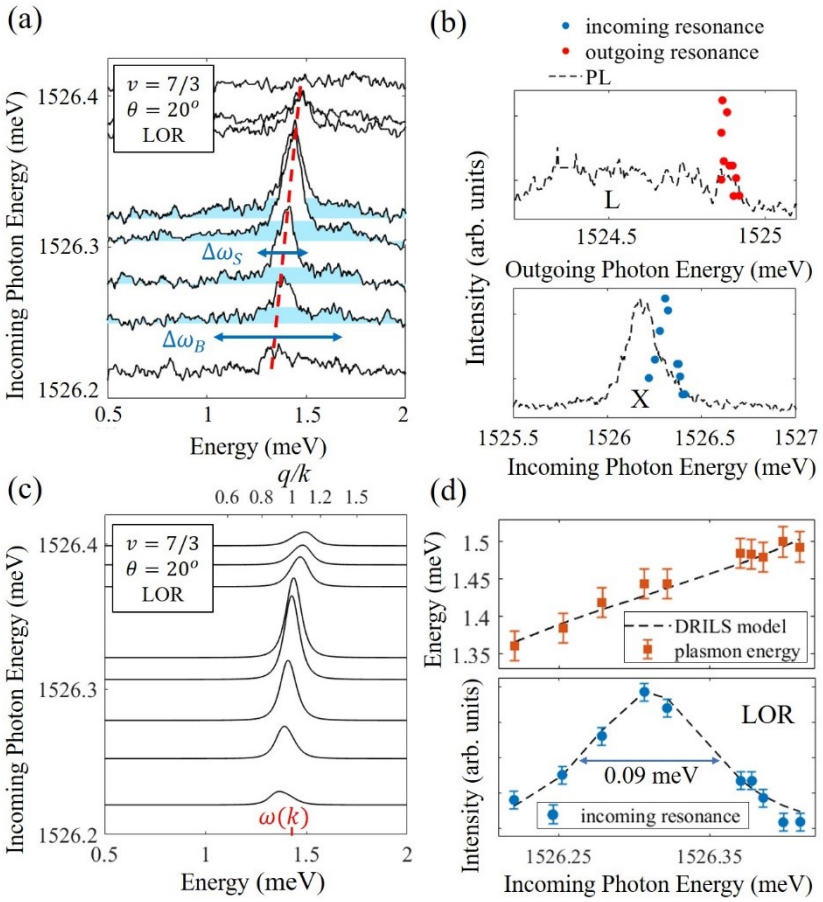


FIG. 2 (color online). (a) DRILS-LOR spectra of nematic plasmon modes measured at $\nu$ = 7/3. The dashed line marks their blueshift. Areas filled in cyan indicate the underlying continuum. Arrows mark the different energy ranges of plasmons and the continuum. (b) Outgoing (top panel) and incoming (bottom panel) resonances of plasmons. (c) LOR plasmon spectra generated by DRILS model, where $(\omega_1, \gamma_1)$ = (1527.31 meV, 0.06 meV), $(\omega_2, \gamma_2)$ = (1524.88 meV, 0.06 meV), $\omega(k)$ = 1.43 meV and $\Delta\omega_S$ = 0.16 meV. The corresponding non-conserved wave vector $q/k$ is labelled on the top x-axis. (d) DRILS model fits (dashed lines) of plasmon energies (top panel) and incoming resonance (bottom panel) using the parameters above. The width of incoming resonance is reduced from $2\gamma_1$ due to the impact of plasmon wave vector distribution.

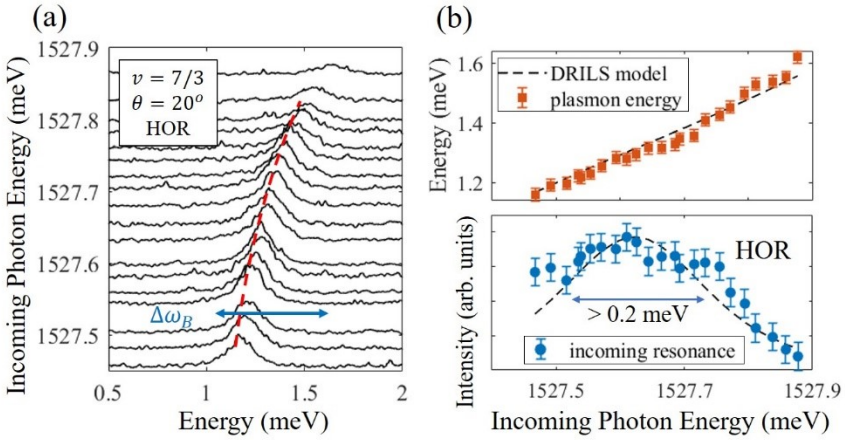


FIG. 3 (color online). (a) DRILS-HOR spectra of nematic plasmon modes within the energy range $\Delta\omega_B$ measured at $\nu$ = 7/3. The dashed line marks their blueshift. (b) DRILS model fits (dashed lines) of plasmon energies (top panel) and incoming resonance (bottom panel) in HOR, where $(\omega_1, \gamma_1)$ = (1527.61 meV, 0.25 meV), $(\omega_2, \gamma_2)$ = (1526.31 meV, 0.06 meV), $\omega(k)$ = 1.32 meV and $\Delta\omega_B$ = 0.35 meV (lower limit). The incoming resonance overlaps $X$+ transitions in PL, which may be a superposition of several optical excitons.

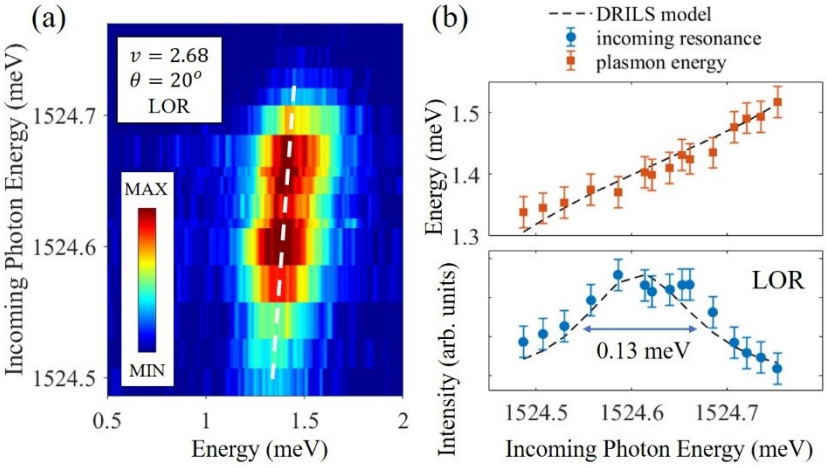


FIG. 4 (color online). (a) DRILS spectra of nematic plasmon modes at $\nu$ = 2.68. The dashed line marks their blueshift. (b) Reproduction of plasmon energy (top panel) and incoming resonance (bottom panel) by DRILS model, where $(\omega_1, \gamma_1)$ = (1524.6 meV, 0.08 meV), $(\omega_2, \gamma_2)$ = (1523.21 meV, 0.08 meV), $\omega(k)$ = 1.41 meV and $\Delta\omega$ = 0.24 meV. The color code is linear with intensity.